Supplementary Information

A Flexible Solid-State Supercapacitor with Extreme Low-Temperature Tolerance Based on Ionic Conducting Ice Gel Electrolytes

Juan. Tu[1], Jia Pan[2], Xinghuan Liu[1], Yinhao Yan[1], Yulin Shi[1], Xinghai Yu[3,] and Xin Jia[1,*]*

[1] School of Chemistry and Chemical Engineering, Shihezi University, Shihezi 832003, China

[2] Department of Chemical and Biomolecular Engineering, University of Delaware Newark, Delaware 19716, USA

[3] College of Chemistry and Chemical Engineering, Hexi University, Zhangye 734000, China

Correspondence to: Xinghaiyu@hxu.edu.cn (X. Yu); jiaxin@shzu.edu.cn(X. Jia)

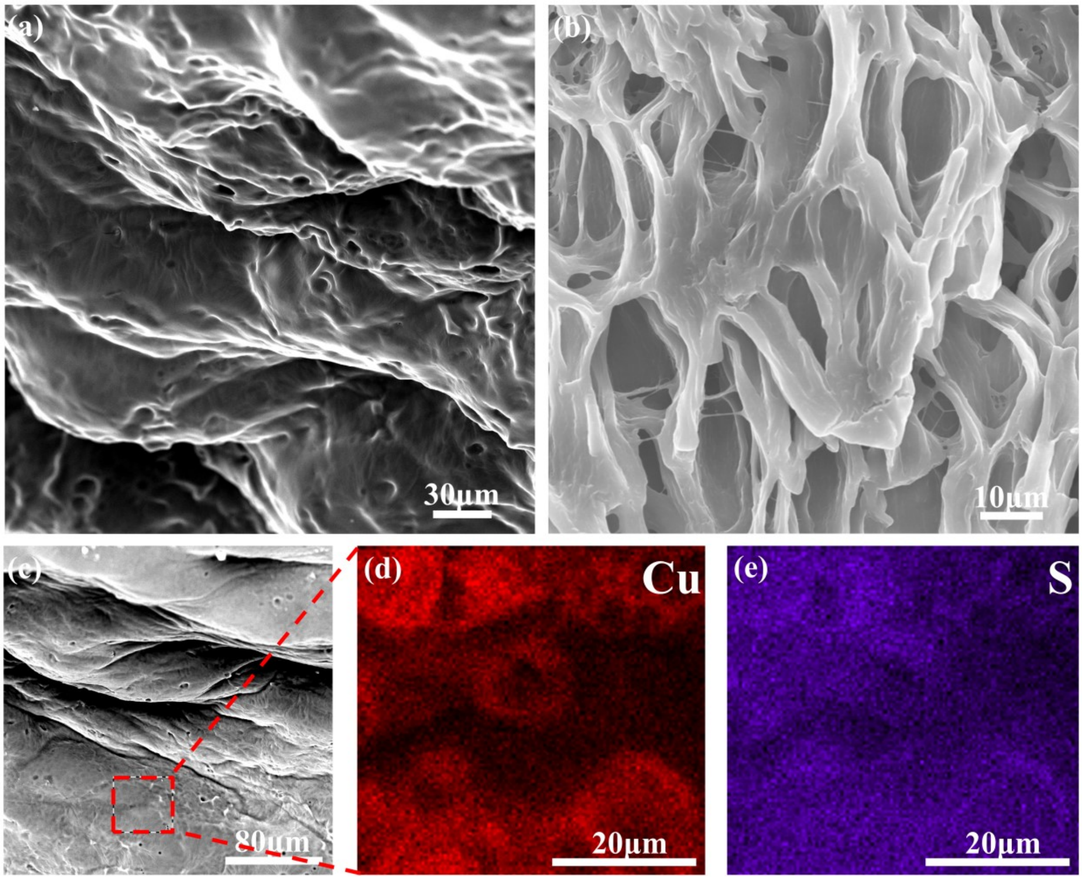

Figure S1. SEM images of freeze-dried IGs containing 1.64 mol L^{-1} $CuSO_4$. (a) Surface image. (b) Cross-sectional image. (c) EDS mapping on selected area of IGs . (d) Cu distribution in the selected area. (e) S distribution in the selected area.

Table S1. The ionic conductivity of the IGs with different concentrations of $CuSO_4$ at -15°C.

$CuSO_4$ concentration (mol L^{-1})	Ionic Conductivity (S cm^{-1})
0.00	1.68×10^{-5}
0.10	3.13×10^{-5}
0.50	3.34×10^{-5}
1.00	4.41×10^{-5}
1.64	1.79×10^{-4}

Table S2. The ionic conductivity of the ice gels with 1.64 mol L^{-1} of $CuSO_4$ at different temperatures.

Temperature (°C)	Ionic Conductivity (S cm^{-1})
25	7.75×10^{-3}
10	5.54×10^{-3}
0	4.79×10^{-3}
-10	3.55×10^{-3}
-20	1.4×10^{-4}
-30	0.98×10^{-6}
-40	0.9×10^{-6}
-50	0.58×10^{-6}
-60	0.28×10^{-6}
-70	0.14×10^{-6}

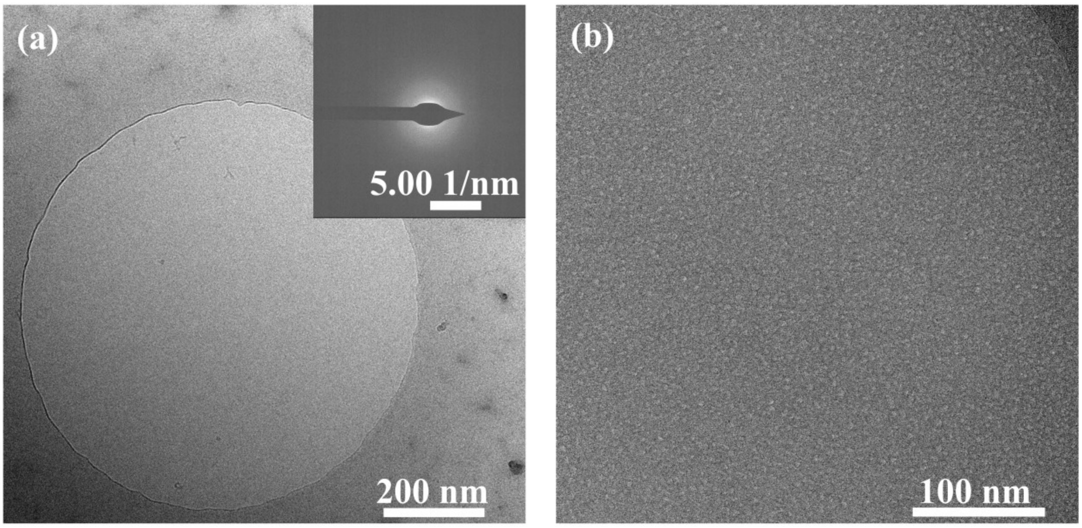

Figure S2. (a), (b) Cryo-TEM micrograph of IGs at low and high magnifications, respectively.

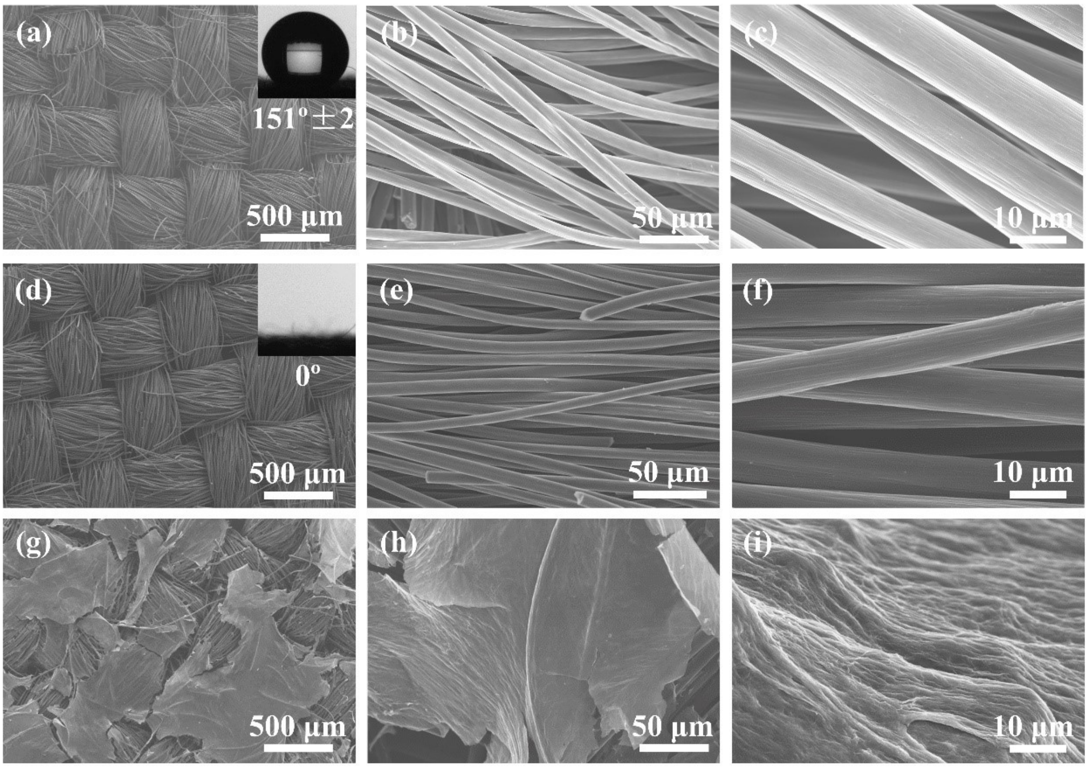

Figure S3. (a), (b) and (c) SEM images of carbon cloth used acid at low and high magnifications, respectively. Inset : liquid-state static contact angle of the carbon cloth. (d), (e), (f), SEM images of the carbon cloth treated with ultraviolet ozone at low and high magnifications, respectively. Inset : liquid-state static contact angle of the carbon cloth. (g) (h), (i), SEM image of RGO loaded on carbon cloth treated with ultraviolet ozone after HTR for 48 hours at low and high magnifications, respectively.

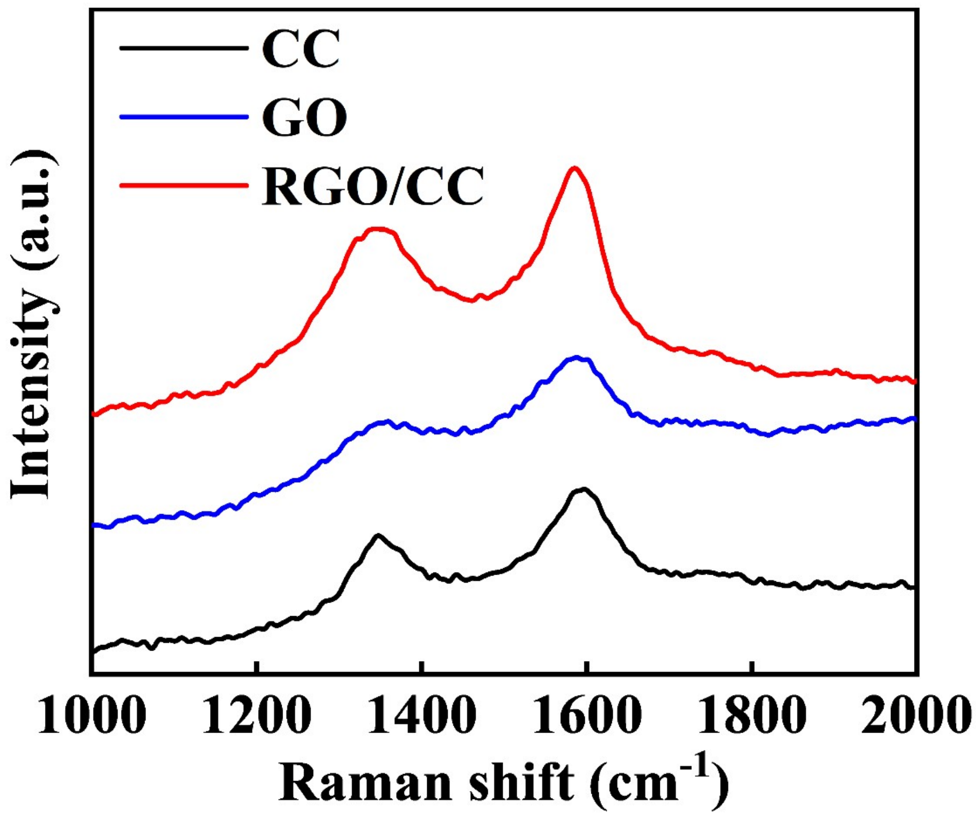

Figure S4. Raman spectra of CC, GO and RGO/CC.

Table S3. D and G peak centres and I_D/I_G for CC, GO, RGO/CC.

Sample	D peak	G peak	I_D/I_G
CC	1347	1597	0.81
GO	1348	1587	0.88
RGO/CC	1345	1585	0.98

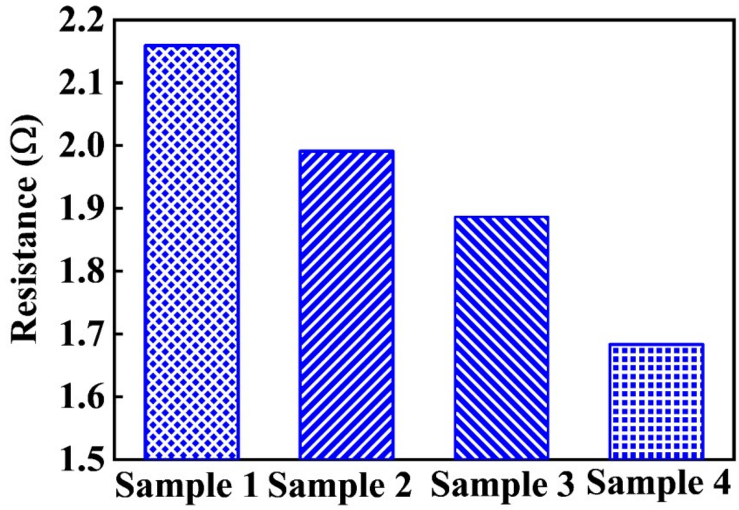

Figure S5. Resistance measurements of the CC electrode and RGO/CC composite electrodes. Sample 1 is pure CC electrode; Sample 2 is the RGO/CC composite electrode after THR treated 48 h without UVO treatment; Sample 3 and 4 are the RGO/CC composite electrodes with UVO treatment, after then treated by THR for 24 and 48 h, respectively.

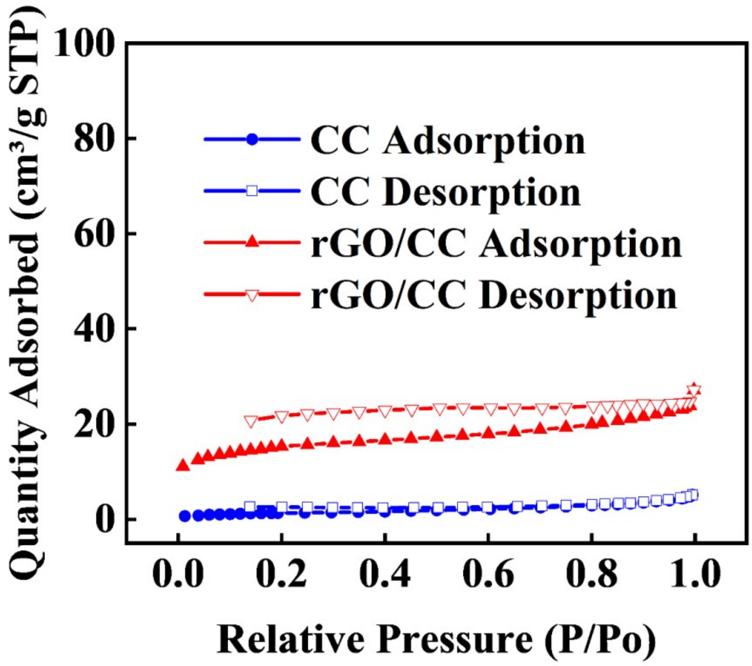

Figure S6. Nitrogen adsorption-desorption isotherm curves of the CC electrode and RGO/CC composite electrode respectively.

Table S4. BET surface area of different electrodes

Sample	S_{BET} (m^2 g^{-1})
CC	4.69
RGO/CC	50.72

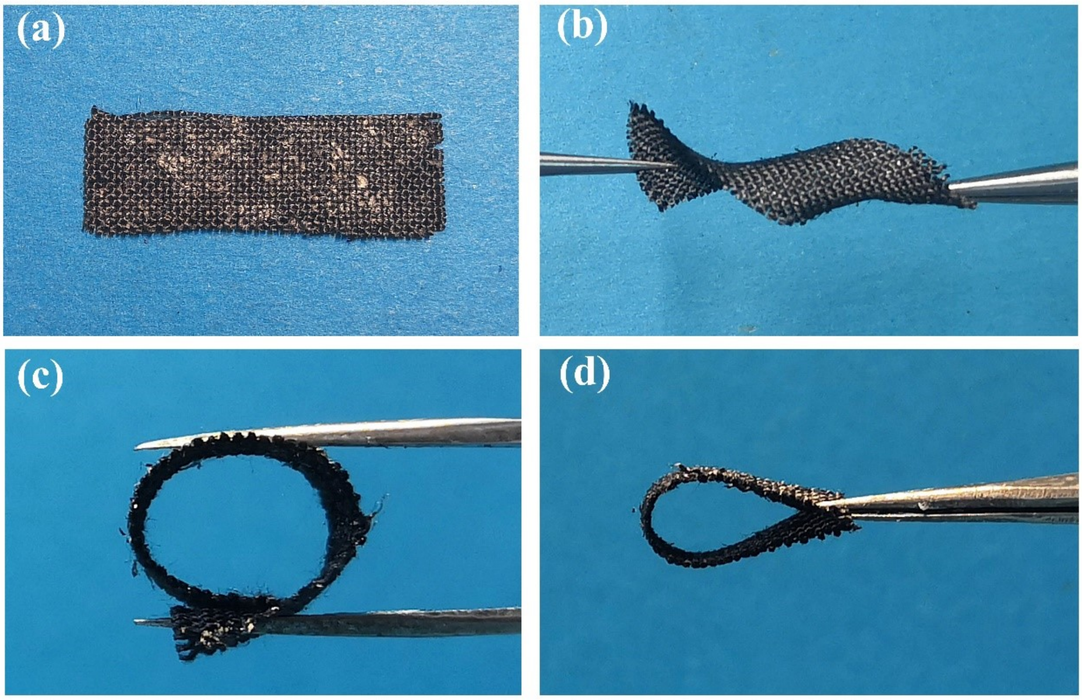

Figure S7. Photographs of the the RGO/CC composite electrode under a variety of deformations.

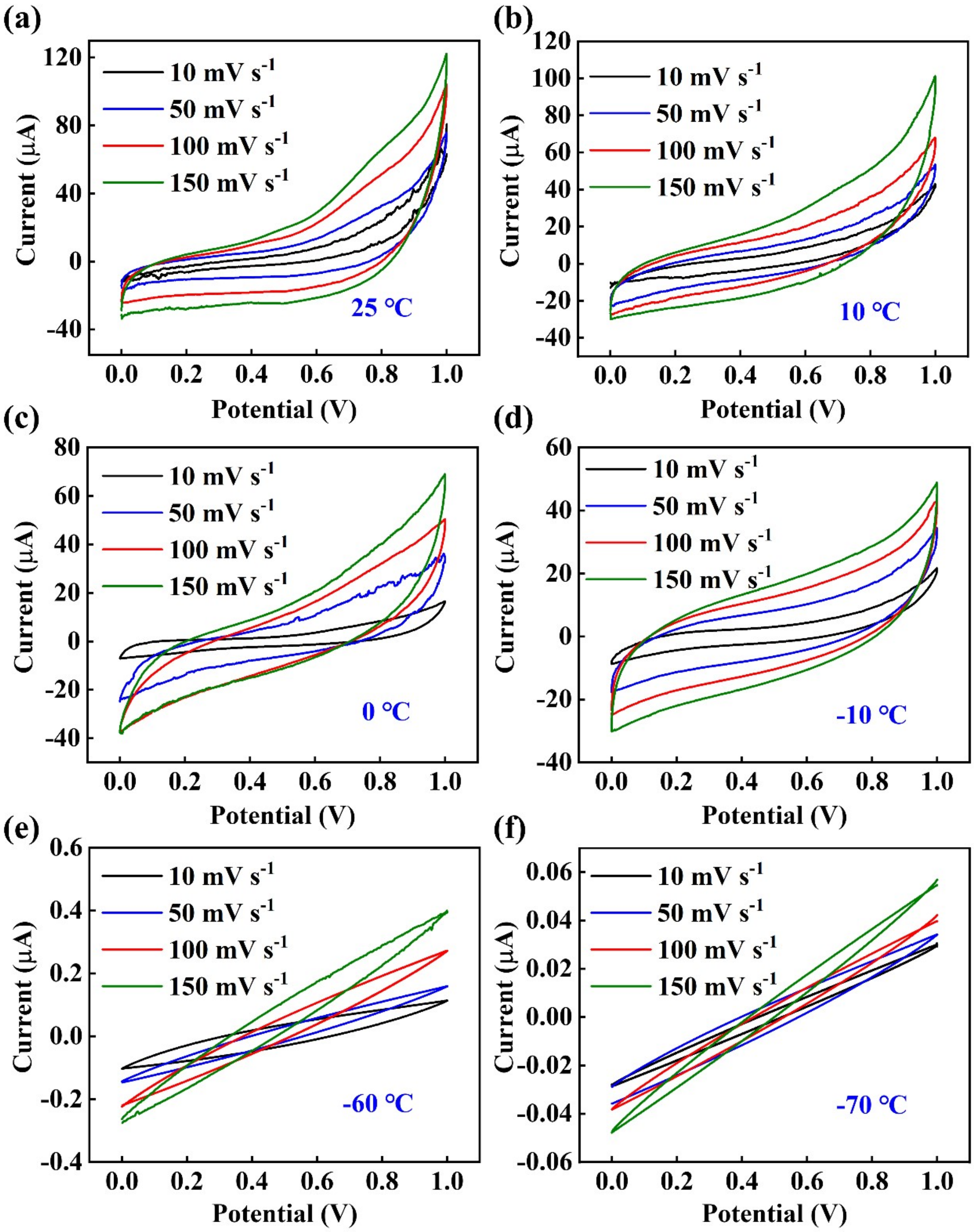

Figure S8. CV curves of the IGs-based supercapacitor at different temperature of 25, 10, 0, -10, -60 and -70 °C, respectively.

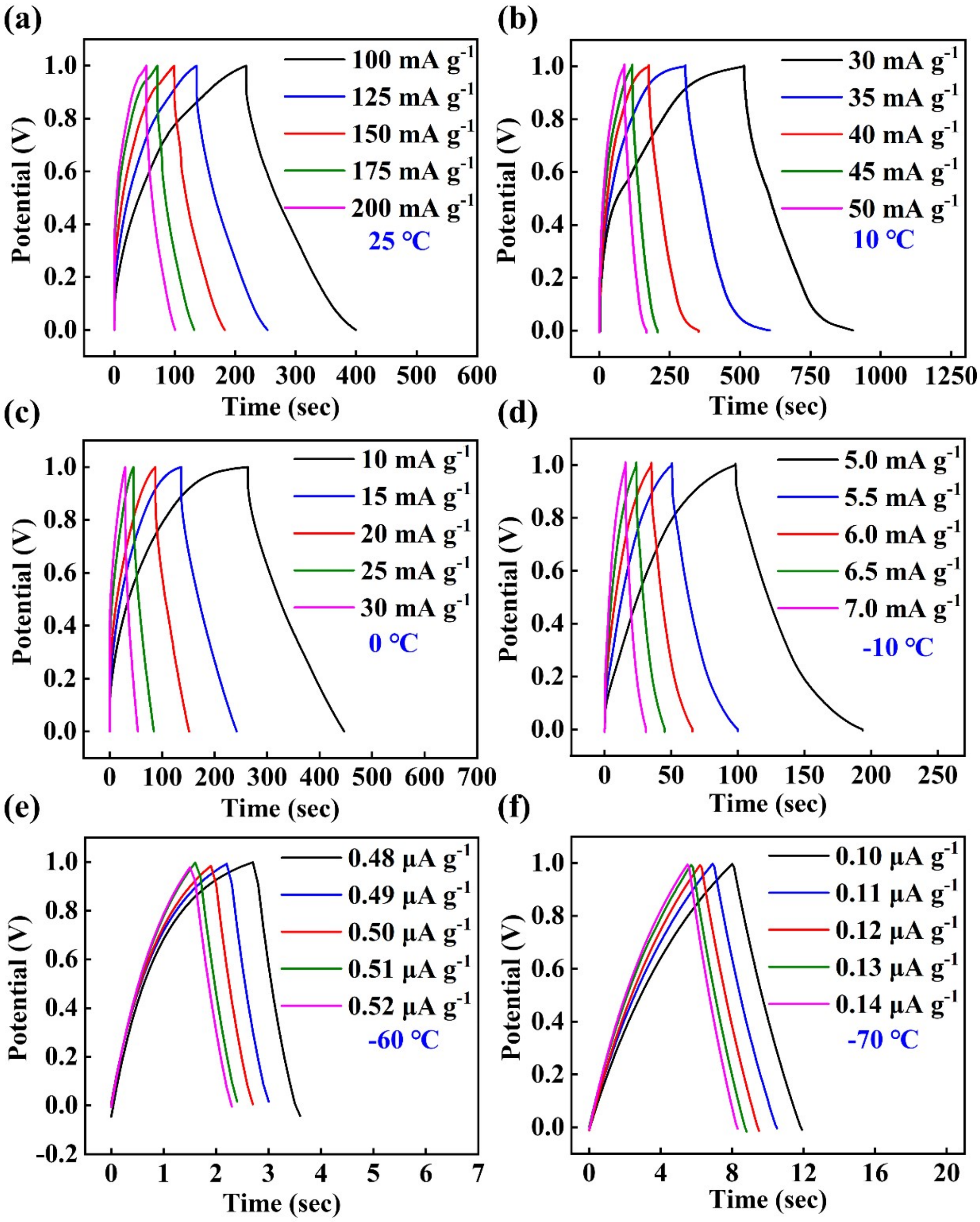

Figure S9. GCD curves of the IGs-based supercapacitor at different temperature of 25, 10, 0, -10,-60 and -70 °C, respectively.

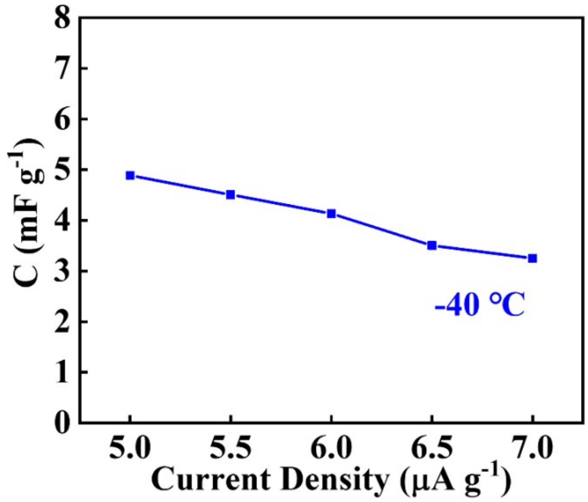

Figure S10. Capacitances at various current densities at -40 °C.

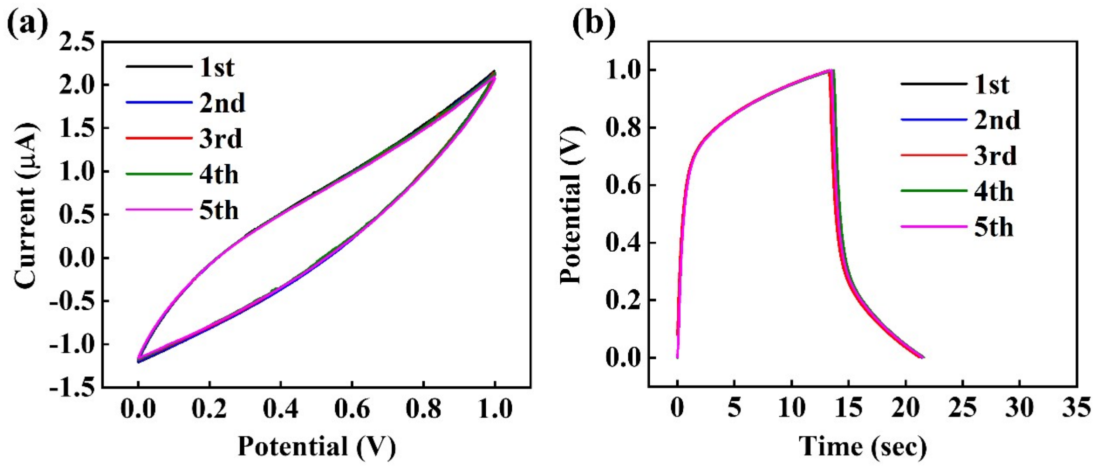

Figure S11. CV (a) and GCD curves (b) with various freezing-thawing cycles. (100 mVs^{-1} scan rate and 30 $\mu A\ g^{-1}$ current density, respectively).

Table S5. The specific capacitances at different temperature.

Temperature (°C)	Current Density (mA g^{-1})	Capacitance (F g^{-1})	ESR Ω
25	100	72.62	71.2
10	30	46.43	11.5
0	10	7.34	455
-10	5	1.89	603
-20	0.1	0.03	4.65×10^{4}
-30	0.01	7.79×10^{-3}	1.73×10^{6}
-40	5×10^{-3}	4.89×10^{-3}	2.91×10^{6}
-50	2.5×10^{-3}	4.90×10^{-4}	3.19×10^{6}
-60	4.8×10^{-4}	1.66×10^{-6}	1.10×10^{7}
-70	1×10^{-4}	1.31×10^{-6}	1.75×10^{7}
-80	4×10^{-5}	1.04×10^{-6}	1.88×10^{7}

Table S6. The specific energy and specific power of the supercapacitor at different temperature.

Temerature (°C)	Energy density (Wh kg^{-1})	Power density (W kg^{-1})	Energy density (Wh cm^{-2})	Power density (W cm^{-2})
25	10.08	199.96	0.13	2.55
10	6.48	60.14	0.083	0.77
0	1.02	19.99	0.013	0.25
-10	0.27	10.09	3.40×10^{-3}	0.13
-20	4.18×10^{-3}	0.20	5.32×10^{-5}	2.55×10^{-3}
-30	1.08×10^{-3}	0.02	1.38×10^{-5}	2.55×10^{-4}
-40	6.79×10^{-4}	0.01	8.64×10^{-6}	1.27×10^{-4}
-50	6.8×10^{-5}	5.00×10^{-3}	8.66×10^{-7}	6.36×10^{-5}
-60	2.50×10^{-7}	1.00×10^{-3}	3.18×10^{-9}	1.27×10^{-5}
-70	1.84×10^{-7}	2.00×10^{-4}	2.35×10^{-9}	2.56×10^{-6}

Table S7. The fitted values of R_S and R_{ct} of supercapacitor.

Temperature(°C)	25	10	0	-10	-20	-30
$R_s(\Omega)$	4.21	5.85	10.81	12.1	370	1.64×10^3
$R_{ct}(\Omega)$	18.64	90.51	460	770.1	1.19×10^3	2.80×10^3

temperature(°C)	-40	-50	-60	-70
Rs(Ω)	5.62×10^3	2.71×10^4	5.05×10^4	6.93×10^4
Rct(Ω)	1.82×10^4	1.36×10^6	2.41×10^6	3.34×10^6